Available online at www.sciencedirect.com
ScienceDirect
Journal of the Mechanics and Physics of Solids
55 (2007) 1298–1320

JOURNAL OF THE MECHANICS AND PHYSICS OF SOLIDS

www.elsevier.com/locate/jmps

Breakage mechanics—Part II: Modelling granular materials

Itai Einav*

School of Civil Engineering, J05, The University of Sydney, Sydney, NSW, 2006, Australia

Received 5 July 2006; received in revised form 19 October 2006; accepted 6 November 2006

Abstract

The compression of granular materials has been traditionally modelled with the limitations of classical elasto-plasticity. The energy was implicitly assumed to dissipate from the frictional interaction of particles. However, the fact that brittle granular materials crush suggests that energy must also be dissipated from the fracturing of the grains, as in fracture mechanics. The concept of breakage as a thermomechanical internal variable was introduced in Part I [Einav, I., 2006. Breakage mechanics—Part I: theory. J. Mech. Phys. Solids 00,000–000] to describe the fracturing mechanisms. The theory allows to treat ideal theoretical materials that undergo dissipation purely from breakage with no other mechanism allowed for the energy consumption. However, as accounted for in elasto-plasticity, dissipation must also occur from the frictional rearrangement of grains. The combination of the two dissipative mechanisms of breakage and plasticity must therefore be investigated, as we do in this paper. Those two mechanisms are generally coupled, in the sense that one inevitably appears when the other develops. Plastic dissipation emerges as a by-product of breakage dissipation because after grains crush, local rearrangement must occur. This scenario may be termed an 'active breakage mechanism', and typifies compression deformations. In shear the plastic dissipation is dominant but breakage appears inevitably from grains abrasion. This scenario may be called a 'passive breakage mechanism'. Based on the coupling assumption, models are developed for granular materials. In particular, we show that in compression isotropic hardening of sands may appear without involving plastic strains, i.e., independent of frictional dissipation. This interpretation of hardening is different from the one used in classical critical state soil mechanics.

*Tel.: +612 935 12113; fax: +612 935 13343.
E-mail address: i.einav@civil.usyd.edu.au.

0022-5096/$ - see front matter
doi:10.1016/j.jmps.2006.11.004

However, frictional dissipation leads to plastic straining that are necessary for the models to be predictive in unloading.

Keywords: Granular materials; Breakage; Plasticity; Micromechanics; Dissipation

1. Introduction

Since the number of flaws within particles is relative to their sizes, the collective behaviour of the sand agglomerate is isotropically strength hardening under compression as particles get smaller (e.g., McDowell et al., 1996). Isotropic hardening was linked to the fracturing of particles and the creation of new surface area by introducing the concept of clastic hardening and separating between dissipation from fracture and plasticity (McDowell and Bolton, 1998). The fracture term, however, was degenerated into the usual plastic dissipation term for a particular one-dimensional consolidation loading case. This does not allow the clastic hardening theory to be developed further for other loading conditions that may apply to the material. In this paper we analogously show that isotropic hardening may be related to the growth of breakage in Continuum Breakage Mechanics (CBM) models, parallel to the effect of increasing surface area. In doing so, we strengthen the conclusion that isotropic hardening is indeed related to fracture type of dissipation rather than to plastic dissipation. However, the CBM theory allows developing "complete" models. By "complete" we mean models that predict the behaviour of crushable granular materials under different loading conditions, such that it would be possible to integrate them in finite element programs.

The growth of breakage describes the evolution of the grain size distribution from an initial to ultimate distributions. In Part I (Einav, 2006) of this paper we incorporated the concept of breakage as an internal variable in a thermomechanical analysis and developed the theory for constructing CBM models. The theory allows to treat ideal theoretical materials that purely undergo dissipation from breakage with no other mechanism allowed for the energy consumption. We cannot neglect, however, that additional dissipation in granular materials arises from frictional rearrangement. The frictional dissipation is most efficiently described in terms of the conventional dissipation of plasticity. The combination of the two dissipative mechanisms of breakage and plasticity must therefore be investigated, as we do in this paper.

Those two mechanisms are generally coupled, in the sense that one inevitably appears when the other develops. Plastic dissipation emerges as a by-product of breakage dissipation because when grains crush local rearrangement must occur. This scenario may be termed an 'active breakage mechanism', and typifies compression deformations. In shear the plastic dissipation is dominant but breakage appears inevitably from grains abrasion. This scenario may be called a 'passive breakage mechanism'. Based on the coupling assumption the CBM theory is taken further, and models are developed for granular materials. In particular, we show that in compression isotropic hardening of sands may appear without involving plastic strains, i.e., independent of plastic dissipation. This interpretation of hardening is therefore different from the one used in classical critical state soil mechanics. However, plastic dissipation leads to plastic straining that are necessary for the models to be predictive in unloading.

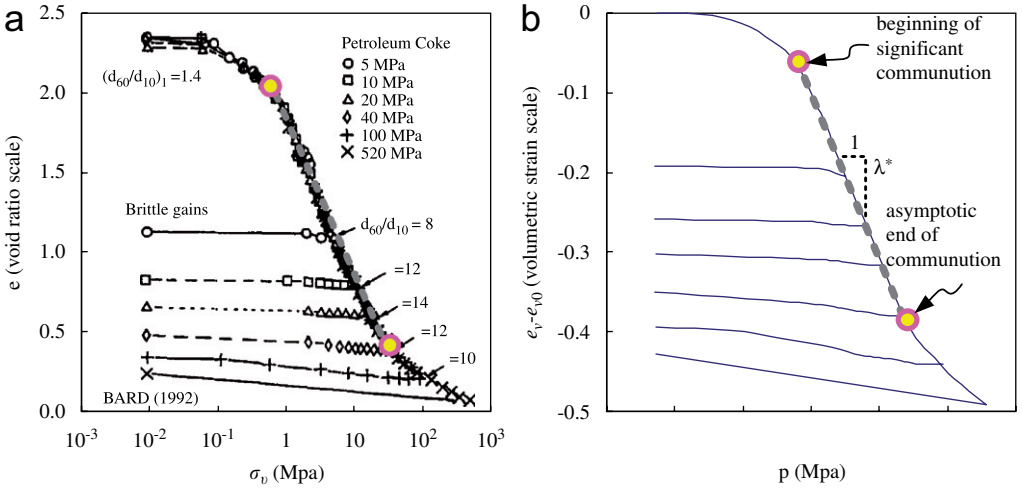

Fig. 1. One-dimensional cyclic compression test presented in either (a) e−log(σ_v) plot (after Biarez and Hicher, 1994) or (b) e_v−log(p) plot (re-plotted figure).

1.1. Compression of sand

In critical state soil mechanics plastic strains are assumed to commence when the mean effective stress, p, meets the "pre-consolidation pressure", p_y, under isotropic ($q = 0$) compression conditions. In the early developments of critical state soil models for remoulded clays (Schofield and Wroth 1968; Roscoe and Burland 1968), the pre-consolidation pressure was expressed purely using the specific volume $v = 1 + e$ (with e being the void ratio). In these models the normal compression curve ($p = p_y$) was assumed to be linear in e–log(p) space, with a slope designated by λ.[1] A more recent suggestion is to express linearity between the pre-consolidation pressure and the void ratio in log–log space (e.g., Butterfield, 1979), i.e., a linear relation between log(p) and log(1 + e). The increments of the volumetric strain δe_v and void ratio δe can be approximated by $\delta e_v = \delta e/(1 + e)$, so for a linear relation in log(v)−log(p), the linearity may also be assumed in e_v−log(p) with a modified slope λ^* in space. For clays, the initial volumetric strain may be assumed by $e_{v0} = \log(v_\lambda/v_0)$ (Einav and Carter, 2007), where v_λ signifies the specific volume at the reference pressure. The merging of p with p_y when plastic straining commences, and the linearity of the compression curve in e−log(p) space, was shown to be suitable for sand as well as other crushable aggregates (Novello and Johnston, 1989).

Fig. 1(a) demonstrates a typical one-dimensional cyclic compression plot for petroleum coke by Biarez and Hicher (1994). The plot also shows values of uniformity coefficient increasing to a constant value at lower void ratios, in which stage the curve starts to be concave. The point is schematically added in the figure. McDowell et al. (1996) suggest that this in effect marks the possible limit of comminution, added to the fact that void ratios cannot be negative. The end of the comminution may in return be linked to the asymptotic

[1]Not to be confused with the 'non-negative plasticity multiplier' which will be used later.

approach of breakage towards one, hence the infrequency of crushing events. Before moving towards the asymptotic end of comminution, the curve is indeed fairly linear as assumed in critical state soil mechanics. Fig. 1(b) re-plot the same curve in e_v–log(p) space, showing linearity over a wide range of stresses with a slope being marked as λ^*. The analysis in this paper is limited to represent the behaviour before going out of the upper limit of the comminution domain.

The usual modelling scheme in critical state soil mechanics is to measure λ (or λ^*), phenomenologically, directly from the curve, and impose the linear relation in the e–log(p) space (or the e_v–log(p) space) when developing models. This does not allow, for example, to predict any change in the behaviour when the grain size distribution or other physical parameters change. Instead, any change needs recalibration of the parameter λ. Can we find a more rational way?

In this paper we follow a more recent approach, that was originally undertaken by McDowell et al. (1996). In this approach the physical reasons to the logarithmic linearity is sorted out rather than ignored. However, unlike McDowell et al's work, we end up not only with a conceptual explanation, but follow a 'rigorous' procedure and the models can be 'operational'. In 'rigorous' we mean that the evolution equations can be derived based on a modern thermomechanical procedure. In 'operational' we mean that models may predict the soil response for any loading conditions, using a new mathematical framework (the Theory of CBM). In doing so, the current work provides the first consistent method to asses the effect of grain size distribution, and the way it evolves, on the stress–strain response of the material.

2. Pure elastic-breakage theory

In Part I of this paper the new theory of CBM was presented. The theory was limited for pure elastic-breakage models (total strain is also the elastic strain $e = e_e$). An emphasize was placed to the fact that the theory provides a direct physical interpretation to the different internal variables. The entire constitutive response of CBM models may be consistently derived by following a thermomechanical procedure. In the following we present a brief description of the theory, referring to equations from Part I by the notation $\mathrm{P_I}(x)$, where 'x' refers to the equation number from Part I. It is also convenient to replace total strain symbol e, from Part I, by the elastic strain symbol e_e because this will enable us to extend the study for elastic-plastic-breakage models in ease.

2.1. Helmholtz free energy

The general structure of pure elastic-breakage Helmholtz free energy is given by ($\mathrm{P_I}(26)$)

$$\Psi \equiv \psi_r(e_e)[(1-B)m_0 + Bm_u]. \tag{1}$$

Taking the reference grain size as $d_r = \sqrt{J_{20}}$ (see $\mathrm{P_I}(41)$), then for a system of spheres

$$\Psi \equiv \psi_r(e_e)(1-\vartheta B), \tag{2}$$

where using $m_0 = 1$ and $m_u = J_{2u}/J_{20}$ (see $\mathrm{P_I}(46)$), we designate

$$\vartheta = 1 - \frac{J_{2u}}{J_{20}}. \tag{3}$$

We note that $1 \geqslant \vartheta \geqslant 0$. The second order moments of the initial and ultimate grain size distributions, $p_0(d)$ and $p_u(d)$, are given by applying $P_I(19)$:

$$J_{20} \equiv \langle d^2 \rangle = \int_{d_m}^{d_M} d^2 p_0(d)\,\mathrm{d}d, \tag{4}$$

$$J_{2u} \equiv \langle d^2 \rangle = \int_{d_m}^{d_M} d^2 p_u(d)\,\mathrm{d}d. \tag{5}$$

Therefore the parameter ϑ measures the proximity of the initial to ultimate grain size distributions.

For example, assuming that the ultimate distribution is fractal (see $P_I(A.11)$ and $P_I(35)$)

$$J_{2u} = \frac{3-\alpha}{5-\alpha} d_M^2. \tag{6}$$

The stress is given by differentiating Eq. (2) with respect to the elastic strain as

$$\sigma = \psi_r'(e_e)(1 - \vartheta B), \tag{7}$$

where $\psi_r'(e_e) = \partial \psi_r(e_e)/\partial e_e$. Using Eqs. (3) and $P_I(36)$ and $P_I(53)$, we write the 'breakage energy' and 'residual breakage energy' by

$$E_B = \vartheta \psi_r(e_e), \tag{8}$$

$$E_B^* = E_B(1-B) = (1-B)\vartheta \psi_r(e_e). \tag{9}$$

2.2. Breakage growth and dissipation

In $P_I(57)$ the following yield criterion was adopted:

$$y_B(B, E_B) = E_B(1-B)^2 - G_B \leqslant 0 \tag{10}$$

proposing that G_B is a breakage strain energy constant of material. The breakage dissipation may be written in two various forms by $P_I(58)$ and $P_I(59a)$:

$$\tilde{\Phi}_B = G_B(1-B)^{-2}\delta B, \tag{11}$$

$$\tilde{\Phi}_B = E_B \delta B = \delta E_B^*. \tag{12}$$

The second form may also be interpreted as a 'breakage growth criterion', stating that energy dissipation from breakage is fully attained from loss in residual breakage energy (see $P_I(59b)$). Fig. 2 portrays the physical meaning of this breakage growth criterion, showing the area linked with the change of the residual breakage energy E_B^*, i.e., δE_B^*. It seems very attractive to postulate that the breakage dissipation will equate δE_B^*, since the associated area represents only those particles that has undergone a change in their size.

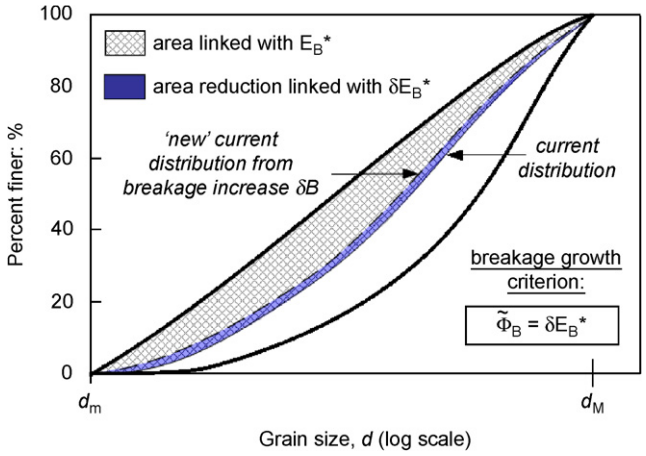

Fig. 2. Schematic representation of the postulate of breakage growth criterion.

3. A pure elastic-breakage compression model

3.1. Mathematical representation

Based on the Helmholtz free energy in the reference grain fraction in Eqs. (A.5) and (A.6), and using Eq. (2), the total Helmholtz free energy of crushable granular materials may be expressed as

$$\Psi = \frac{p_r\left(\xi(e_v^e)/p_r\right)^{2-m}}{\bar{K}(2-m)}(1-\vartheta B) \quad \text{for } 0 \leqslant m < 1, \tag{13}$$

$$\Psi = p_r \kappa^* \exp\left((e_v - e_{v0})/\kappa^*\right)(1-\vartheta B) \quad \text{for } m = 1. \tag{14}$$

The pressure is then modified from that of Eqs. (A.3) and (A.4):

$$p = \xi(e_v^e)(1-\vartheta B) \tag{15}$$

so that only before commencement of breakage (while $B = 0$), the above expression agrees with Eqs. (A.3) and (A.4). The breakage energy is calculated by applying Eq. (8):

$$E_B = \vartheta \frac{p_r\left(\xi(e_v^e)/p_r\right)^{2-m}}{\bar{K}(2-m)} \tag{16}$$

with $\bar{K} = 1/\kappa^*$ when $m = 1$.

Before yielding and commencement of breakage the relation between the pressure and volumetric strain is given by $p = \xi(e_v^e)$, where $\xi(e_v^e)$ is given in Eqs. (A.3) or (A.4). This continues until $E_B = G_B$, from then on breakage develops. The pressure at the commencement of breakage is

$$p_{y0} = p_r \sqrt[2-m]{\frac{G_B \bar{K}(2-m)}{\vartheta p_r}}. \tag{17}$$

when $m=1$, $p_{y0}=G_B(\kappa^*\vartheta)^{-1}$. This 'initial' yield stress is related to the initial pre-consolidation pressure in critical state soil mechanics. Since $\bar{K}$ is a function of the initial void-ratio, and ϑ is a function of the grain sizes, so should the initial pre-consolidation pressure be. This means that p_{y0} depends on the initial state, i.e., initial void ratio e_0 and initial grain size distribution, $p_0(d)$, in agreement with the experimental conclusion by Nakata et al. (2001). However, the strain energy breakage constant G_B is believed to be an average constant of the overall granular assembly (i.e., not of individual grains), and independent of the state. This presents another attractive outcome that this work offers.

After yielding the breakage is given by combining Eq. (16) with Eqs. (10) and (A.3):

$$B=1-\sqrt{\frac{\bar{K}(2-m)G_B}{\vartheta p_r^{m-1}}\xi(e_v^e)^{m-2}}, \tag{18}$$

with $\bar{K}=1/\kappa^*$ when $m=1$. The explicit stress–strain curve is given simply by substituting the last relation in Eq. (15).

3.2. Model behaviour

Fig. 3 presents typical compression stress–strain curves of the pure elastic-breakage model in a semi-logarithmic scale, for a sample with initial void ratio of $e_0=1.5$ and maximum void ratio of $e_{\max}=1.8$. The elastic parameters are taken as $m={}^1/_2$, and $\bar{K}=500$. The breakage strain energy constant, for this figure, is $G_B=10\,\mathrm{kPa}$. The ratio between the ultimate and initial second order moment of the grain size distributions is taken in the range of 0–1 in increments of 0.1, giving ϑ ranging from 1 to 0 with opposite

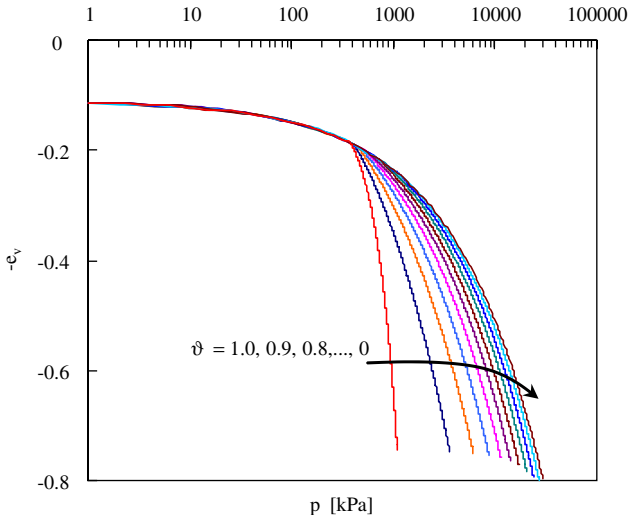

Fig. 3. Effect of grain size distribution on compression curves in pure elastic-breakage model.

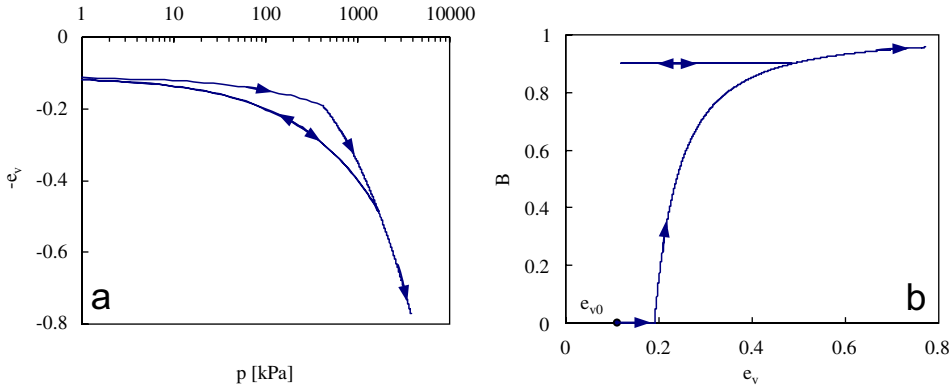

Fig. 4. 'Isotropic hardening' in compression pure elastic-breakage model: (a) stress–strain curve in semi-logarithmic scale and (b) breakage growth against volumetric strain.

increments. As ϑ gets smaller, the potential of the grains to crush reduces, presenting a less dramatic change in the curve. Furthermore, the initial yield pressure, p_{y0}, increases according to Eq. (17), until it tends to infinity when $\vartheta = 0$. In these conditions, which represents a situation where the initial grain size distribution is already the ultimate one, breakage will not develop.

Fig. 4(a) presents the corresponding loading–unloading–reloading compression curve for the same theoretical material with $\vartheta = 0.9$. For the breakage strain energy constant of $G_B = 10\,\text{kPa}$, the initial pre-consolidation pressure is $p_{y0} = 411\,\text{kPa}$. Fig. 4(b) presents the growth of breakage with volumetric strain. As is seen, the breakage remains constant during unloading. In reloading, it remains constant until the sample yields again, but at a higher pressure value than p_{y0}. Then the breakage continues to growth again, asymptotically towards one. The fact that the yielding point increases from its initial p_{y0} value, with breakage, gives an alternative physical explanation to the so-called 'isotropic hardening' in granular materials. This is in accord with McDowell et al. (1996). The increase in the pre-consolidation pressure is directly viewed as the outcome of grain fracture, growth of surface area, and breakage. From CBM view point, the yield strength increases because the grain size distribution is shifting gradually towards smaller particles. Since fragmented particles store less strain energy than the originally bigger particles (see details in Part I of the paper, where the energy split hypothesis is introduced), more straining is needed to attain the same breakage criterion (and getting back to the same strain energy constant). In other words, the overall aggregate is isotropically breakage hardening.

The unloading elastic modulus degrades with the growth in breakage, such that upon unloading back to the reference pressure p_r, the volumetric strain returns to its initial value, without any plastic strains. It is widely accepted, however, that sands undergo residual strains in this loading scenario, so that predictive models must include further dissipation from friction. The frictional dissipation is most efficiently described in terms of the conventional plastic dissipation of plasticity. The combination of the two dissipative mechanisms of breakage and plasticity must therefore be investigated, as we do in the next section. We note that the secondary compression curve in this pure elastic-breakage

model is non-linear in this plot, while the typical curve in Fig. 1(b) presents linearity when comminution occurs. As we shall see, the addition of plastic dissipation can adjust this deviation.

4. Elastic–plastic-breakage formulation

The constitutive behaviour of brittle granular materials would mostly relate to two general dissipative mechanisms: dissipation from plasticity and dissipation from breakage. These two mechanisms are generally coupled in the sense that one inevitably appears when the other develops. Based on the coupling assumption, an elastic–plastic-breakage theory is developed for granular materials. However, we start by presenting the mathematical foundation of plastic dissipation and developing an uncoupled approach. This uncoupled approach will provide a good starting point before advancing to the couple approach.

4.1. Plastic dissipation

The frictional dissipation is most efficiently described in terms of the conventional plastic dissipation of plasticity. For rate independent materials the increment of plastic dissipation is assumed homogeneous first order function of the plastic strain increment

$$\tilde{\Phi}_p(B,\delta e_p) \equiv \frac{\partial \tilde{\Phi}_p(B,\delta e_p)}{\partial \delta e_p} : \delta e_p, \tag{19}$$

where e_p and δe_p are the plastic strain and its increment, and satisfy the cumulative decomposition of strains:

$$e \equiv e_e + e_p, \tag{20}$$

$$\delta e \equiv \delta e_e + \delta e_p. \tag{21}$$

The decomposition assumption is generally regarded as one of the most effective working hypothesizes in soil mechanics. It is important to mention, however, that there are theoretical grounds to question the validity of this hypothesis since the contact law between particles is non-linear in nature, (see Collins and Einav, 2005). Nevertheless, since this assumption has proven useful over the years, let us proceed by adopting it.

4.2. Uncoupled dissipation and two separate yield conditions

The total increment of dissipation potential $\tilde{\Phi}$ is a combination of the plastic $\tilde{\Phi}_p$ and breakage $\tilde{\Phi}_B$ components. In 'uncoupled' models, those two terms are assumed to be additive:

$$\tilde{\Phi} = \tilde{\Phi}_p + \tilde{\Phi}_B \geqslant 0 \tag{22}$$

Considering Eqs. (11) and (19):

$$\tilde{\Phi} = \frac{\partial \tilde{\Phi}}{\partial \delta e_p} : \delta e_p + \frac{\partial \tilde{\Phi}}{\partial \delta B}\delta B, \tag{23a}$$

$$\tilde{\Phi} = \frac{\partial \tilde{\Phi}_p}{\partial \delta e_p} : \delta e_p + \frac{\partial \tilde{\Phi}_B}{\partial \delta B} \delta B. \tag{23b}$$

Combining the last equation with the increment of stored energy in Eq. (2), the incremental decomposition assumption in Eq. (21), and the energy conservation law from $P_I(21)$:

$$\tilde{W} = \delta \Psi + \tilde{\Phi} \tag{24}$$

gives a modify version of $P_I(34)$:

$$\left(\sigma - \psi'(e_e)(1 - \vartheta B)\right) : \delta e_e + \left(\sigma - \frac{\partial \tilde{\Phi}_p}{\partial \delta e_p}\right) : \delta e_p + \left(\vartheta \psi(e_e) - \frac{\partial \tilde{\Phi}_B}{\partial \delta B}\right) \delta B = 0. \tag{25}$$

From which one gets

$$\sigma = \psi'(e_e)(1 - \vartheta B), \tag{26a}$$

$$\sigma = \frac{\partial \tilde{\Phi}}{\partial \delta e_p} = \frac{\partial \tilde{\Phi}_p}{\partial \delta e_p}. \tag{26b}$$

Eq. (26a) is similar to Eq. (7), but this time the stress is also given by Eq. (26b) whenever yielding occurs. This gives rise to plastic strains.

The breakage energy may also be defined in two various forms:

$$E_B = \vartheta \psi(e_e), \tag{27a}$$

$$E_B = \frac{\partial \tilde{\Phi}}{\partial \delta B} = \frac{\partial \tilde{\Phi}_B}{\partial \delta B}, \tag{27b}$$

where the second equation implies breakage growth whenever yielding occurs. Using Eqs. (26b) and (27b), Eq. (23) may be re-written as

$$\tilde{\Phi} = \sigma : \delta e_p + E_B \delta B. \tag{28}$$

As in pure elastic-breakage models, we identify the breakage yield condition:

$$\lambda_B y_B(B, E_B) \equiv E_B \delta B - \tilde{\Phi}_B(B, \delta B) = 0, \tag{29}$$

but unlike the pure elastic-breakage models an additional plastic yield condition could be defined:

$$\lambda_p y_p(B, \sigma) \equiv \sigma : \delta e_p - \tilde{\Phi}_p(B, \delta e_p) = 0, \tag{30}$$

where $y_p(B, \sigma) \leqslant 0$ and $\lambda_p \geqslant 0$.

4.3. Coupled dissipation and a single combined yield condition

A less trivial form of dissipation than Eq. (22) is given by

$$\tilde{\Phi} = \sqrt{\tilde{\Phi}_p^{*2} + \tilde{\Phi}_B^{*2}} \geqslant 0 \tag{31}$$

in a way that maintains the first order dependence of the total dissipation on the increments. The superimposed '*' in $\tilde{\Phi}_p^*$ and $\tilde{\Phi}_B^*$ is added to highlight that those terms are conceptually different than $\tilde{\Phi}_p$ and $\tilde{\Phi}_B$, but are still homogeneous first order functions of

the plastic strain and breakage increments. We note that

$$\frac{\partial\tilde{\Phi}}{\partial\delta e_p}=\frac{\tilde{\Phi}_p^*}{\tilde{\Phi}}\frac{\partial\tilde{\Phi}_p^*}{\partial\delta e_p}, \tag{32}$$

$$\frac{\partial\tilde{\Phi}}{\partial\delta B}=\frac{\tilde{\Phi}_B^*}{\tilde{\Phi}}\frac{\partial\tilde{\Phi}_B^*}{\partial\delta B}, \tag{33}$$

thus it is still possible to show, together with Eqs. (11) and (19), that Eq. (23a) is maintained:

$$\tilde{\Phi}=\frac{\partial\tilde{\Phi}}{\partial\delta e_p}:\delta e_p+\frac{\partial\tilde{\Phi}}{\partial\delta B}\delta B. \tag{34}$$

However, combining this with Eqs. (32) and (33) shows that Eq. (23b) is not satisfied this time. This is due to the coupling between the dissipative mechanisms.

Eq. (25) is therefore slightly modified:

$$\left(\sigma-\psi'(e_e)(1-\vartheta B)\right):\delta e_e+\left(\sigma-\frac{\partial\tilde{\Phi}}{\partial\delta e_p}\right):\delta e_p+\left(\vartheta\psi(e_e)-\frac{\partial\tilde{\Phi}}{\partial\delta B}\right)\delta B=0, \tag{35}$$

thus

$$\sigma=\psi'(e_e)(1-\vartheta B), \tag{36a}$$

$$\sigma=\frac{\partial\tilde{\Phi}}{\partial\delta e_p}=\frac{\tilde{\Phi}_p^*}{\tilde{\Phi}}\frac{\partial\tilde{\Phi}_p^*}{\partial\delta e_p}, \tag{36b}$$

$$E_B=\vartheta\psi(e_e), \tag{37a}$$

$$E_B=\frac{\partial\tilde{\Phi}}{\partial\delta B}=\frac{\tilde{\Phi}_B^*}{\tilde{\Phi}}\frac{\partial\tilde{\Phi}_B^*}{\partial\delta B}. \tag{37b}$$

Again, the pure elastic-breakage relations (7) and (8) are satisfied. However, the dissipative definitions of the stress and breakage energy in Eqs. (36b) and (37b) have been modified compared to Eqs. (26b) and (27b). While the first equality in each of these equations remains similar, the second equalities are multiplied by $\tilde{\Phi}_p^*/\tilde{\Phi}$ and $\tilde{\Phi}_B^*/\tilde{\Phi}$. This is attributed to the dissipative coupling. Any dissipation from plastic straining $\tilde{\Phi}_p^*$ is related to breakage dissipation $\tilde{\Phi}_B^*$.

This means, as opposed to Eqs. (29) and (30), that only a single yield condition may be recovered from the total dissipation $\tilde{\Phi}$. Since the total dissipation is still first order in the increments, a combined Legendre transformation is given by

$$\lambda y\equiv\sigma:\delta e_p+E_B\delta B-\tilde{\Phi}=0. \tag{38}$$

The general form of the yield surface may be extracted by eliminating the plastic strain and breakage increments from Eqs. (36b) and (37b), using (31):

$$y\equiv\frac{\sigma:\sigma}{\left[\partial\tilde{\Phi}_p^*/\partial\delta e_p\right]:\left[\partial\tilde{\Phi}_p^*/\partial\delta e_p\right]}+\left(\frac{E_B}{\partial\tilde{\Phi}_B^*/\partial\delta B}\right)^2-1\leqslant 0. \tag{39}$$

Since $\tilde{\Phi}_p^*$ and $\tilde{\Phi}_B^*$ are first order homogeneous functions, their derivatives are zero order homogeneous functions of the increments, and therefore also the yield function.

The following flow rules are deduced:

$$\delta e_p = \lambda \frac{\partial y}{\partial \sigma} = 2\lambda \frac{\sigma}{\left[\partial \tilde{\Phi}_p^* / \partial \delta e_p\right] : \left[\partial \tilde{\Phi}_p^* / \partial \delta e_p\right]}, \tag{40}$$

$$\delta B = \lambda \frac{\partial y}{\partial E_B} = 2\lambda \frac{E_B}{\left(\partial \tilde{\Phi}_B^* / \partial \delta B\right)^2} \tag{41}$$

both relate to a single non-negative multiplier λ.[2] This suggests that the ratio between the increments of the plastic strain and breakage is given by

$$\frac{\delta e_p}{\delta B} = \frac{\partial y}{\partial \sigma} \Big/ \frac{\partial y}{\partial E_B} = \frac{\sigma}{E_B} \frac{\left(\partial \tilde{\Phi}_B^* / \partial \delta B\right)^2}{\left[\partial \tilde{\Phi}_p^* / \partial \delta e_p\right] : \left[\partial \tilde{\Phi}_p^* / \partial \delta e_p\right]}. \tag{42}$$

Combining the last equation with Eqs. (36b) and (37b) suggests that the ratio between the individual dissipation terms is

$$\left(\frac{\tilde{\Phi}_p^*}{\tilde{\Phi}_B^*}\right)^2 = \frac{\sigma : \delta e_p}{E_B \delta B}. \tag{43}$$

Therefore, the dissipation (31) may be re-expressed alternatively by

$$\tilde{\Phi} = \tilde{\Phi}_B^* \sqrt{1 + \frac{\sigma : \delta e_p}{E_B \delta B}} \geqslant 0, \tag{44a}$$

$$\tilde{\Phi} = \tilde{\Phi}_p^* \sqrt{1 + \frac{E_B \delta B}{\sigma : \delta e_p}} \geqslant 0 \tag{44b}$$

illustrating once again the coupling between the dissipative mechanisms.

Although more subtle than the uncoupled dissipation, the coupled dissipation allows to strongly connect between plastic straining and breakage. Any micro-mechanism that is chiefly in charge of stored energy release from breakage is supplemented by additional energy release from plastic dissipation, and vice versa.

The difference between the two forms of dissipation is given by Eqs. (24) and (31), and illustrated in Fig. 5, where the relations between the total, breakage and plastic dissipation components are plotted. The coupled model seems mathematically more attractive than the uncoupled model, eliminating the corners when $\tilde{\Phi} = \tilde{\Phi}_p$ or $\tilde{\Phi} = \tilde{\Phi}_B$.

[2]Note- λ is conceptually different than the conventional 'plasticity' multiplier λ_p, relating to the increment of breakage as well as the plasticity increment. It should also not be confused with the slope of the secondary compression line, as discussed in Section 1.1.

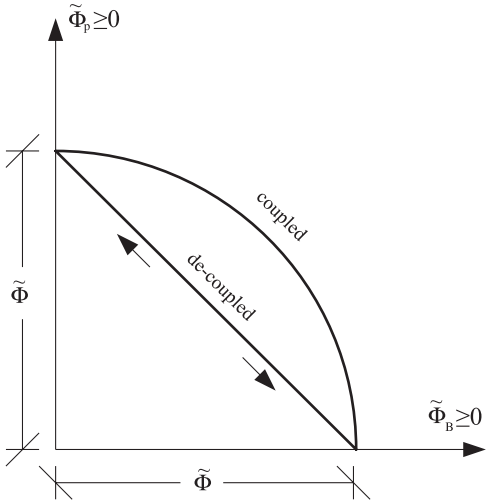

Fig. 5. Schematic representation of uncoupled and coupled dissipations. Note- these lines should not be interpreted as 'yield surfaces'.

5. An elastic–plastic-breakage compression model

In Section 3 a pure elastic-breakage compression model was developed. This model was successful in portraying the physical grounds behind isotropic hardening in sands. However, the pure elastic-breakage compression model is rather limited, from a practical point of view, since upon unloading back to the reference pressure the volumetric strain returns to its initial value without any residual strains (see Fig. 4). This presents a conceptually different behaviour than real granular materials, which do show irrecoverable strains upon unloading (see Fig. 1). The explanation given in the last section is that residual strains may be attributed conventionally as plastic strains, and are due to frictional dissipation from the relative sliding and rolling of the grains in the representative volume element.

A convenient way to develop models is to start with an uncoupled dissipation, then advance it further to a couple model. The ambition in developing models is to be able to follow strong physical concepts that explain soil behaviour effectively. One of such physical concept is based on the postulate of breakage growth criterion (see Paper I). This criterion (see Eq. (12)) requires that the breakage dissipation will equate to the loss in residual breakage energy. The criterion is the outcome of a general yield criterion that was given in Eq. (10). The ambition is then to add plasticity without neglecting this principle. This is achieved by reorganising the definition of plastic dissipation, based on the breakage yield criterion in Eq. (10):

$$\tilde{\Phi}_p = p\delta e_v^p = p\frac{G_B}{E_B(1-B)^2}\delta e_v^p, \tag{45}$$

where we note that $G_B/E_B(1-B)^2 = 1$ when breakage develop. Another way to express this dissipation is given based on the elastic volumetric strain:

$$\tilde{\Phi}_p = \frac{\xi(e_v^e)}{\psi_r(e_v^e)}\frac{(1-\vartheta B)}{(1-B)^2}\frac{G_B}{\vartheta}\delta e_v^p, \tag{46}$$

which with the transformation in Eq. (30) gives the following plastic yield surface:

$$y_p = p - \frac{\xi(e_v^e)}{\psi_r(e_v^e)} \frac{(1-\vartheta B)}{(1-B)^2} \frac{G_B}{\vartheta} \leqslant 0. \tag{47}$$

It is easy to see that with the definitions of $p = \xi(e_v^e)(1-\vartheta B)$, and $E_B = \vartheta \psi_r(e_v^e)$

$$y_p = y_B \tag{48}$$

so the ambition to satisfy the breakage growth criterion in Eq. (12) is trivially satisfied.

To obtain a couple form of total dissipation the individual terms are being factorised by

$$\Phi_p^* = \sin^{-1}(\omega)\Phi_p, \tag{49}$$

$$\Phi_B^* = \cos^{-1}(\omega)\Phi_B, \tag{50}$$

where ω is introduced as the 'plastic-breakage coupling angle', and will be interpreted later on. Substituting these relations in Eq. (39), noting (11) and (46) gives

$$y \equiv \left(\sin(\omega) \frac{\psi_r(e_v^e)\vartheta}{\xi(e_v^e)(1-\vartheta B)} p \right)^2 + (\cos(\omega) E_B)^2 - G_B^2 (1-B)^{-4} \leqslant 0. \tag{51}$$

Since $p = \xi(e_v^e)(1-\vartheta B)$ and $E_B = \psi_r(e_v^e)\vartheta$, the above yield criterion may be reduced to that of a pure elastic-breakage models:

$$y \equiv y_B = E_B - G_B(1-B)^{-2} \leqslant 0, \tag{52}$$

but at the same time to that of the plasticity condition in Eq. (47):

$$y \equiv y_p = p - \frac{\xi(e_v^e)}{\psi_r(e_v^e)} \frac{(1-\vartheta B)}{(1-B)^2} \frac{G_B}{\vartheta} \leqslant 0. \tag{53}$$

With the aid of the consistency condition $\delta y = \delta y_B = 0$, the breakage growth criterion takes the following form:

$$E_B \delta B = \delta E_B^* \tag{54}$$

preserving the second equality of Eq. (12).

We are therefore left with the interpretation of the 'plastic-breakage coupling angle' ω. Before attempting to link this parameter to physical properties, a simple sensitivity analysis is useful. Fig. 6 shows the effect of the coupling angle ω on the compression curves for $e_0 = 1.5$, $e_{\max} = 1.8$, $\vartheta = 0.8$, $m = {}^1/_2$, $\bar{K} = 3000$, and $G_B = 10\,\text{kPa}$. The deviation of the pure elastic-breakage line from the pure elastic line was explained in Fig. 3, and is due to the difference between the initial and ultimate grain size distribution via ϑ. The shift from the pure elastic-breakage line to the pure elastic-plastic line is spanned via the coupling angle ω.

When ω becomes bigger than about 60–70°, the behaviour is essentially linear in the e_v–$\log(p)$ space. This type of linearity agrees with the experimental results in Fig. 1(b), and adjusts the non-linear elastic-breakage line.

Fig. 7(a) shows how the breakage develops with applied volumetric strain. Although the evolution with increase in volumetric strain (or void ratio) depends on the coupling parameter ω, the way it evolves with applied pressure is independent of this parameter.

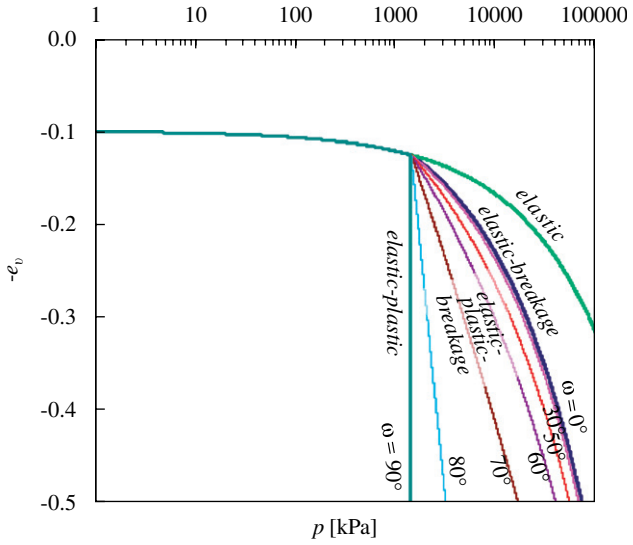

Fig. 6. The coupling effect on the stress–strain curve in semi-logarithmic scale.

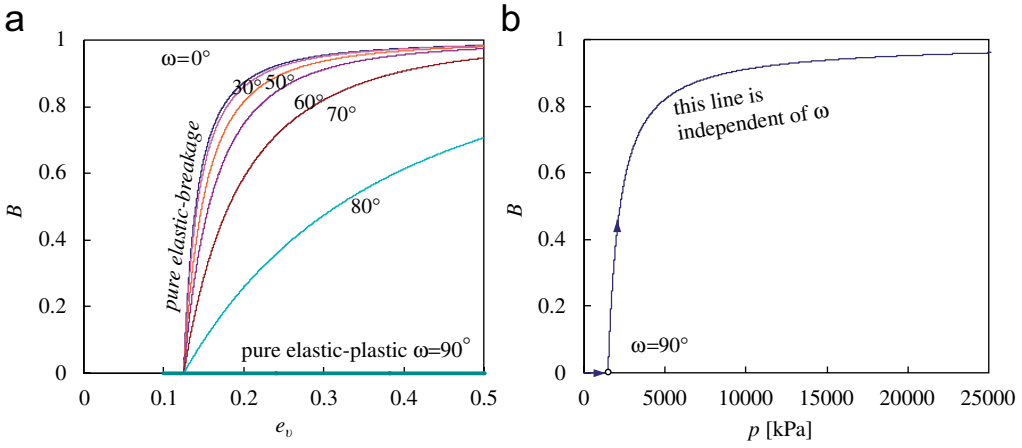

Fig. 7. The coupling effect on breakage growth against volumetric strain and pressure.

This relation is found by combining Eqs. (15), (16) and (53):

$$p = p_{y0}\frac{(1-\vartheta B)}{\sqrt[2-m]{(1-B)^2}} \tag{55}$$

and plotted in Fig. 7(b).

The first term of the yield surface in Eq. (51) vanishes when $\omega = 0^\circ$, and the model reduces to be of purely elastic-breakage type. This corresponds to a zero intergranular

contact friction angle. As ω gets larger, the material shows more plastic strains for the same amount of total strain. When $\omega = 90^\circ$ the yield surface in Eq. (51) looses its second term, and the model becomes essentially elastic-perfectly-plastic. This extreme case may be the situation when the intergranular contact friction coefficient is extremely large, in which case the fracturing dissipative mechanisms (or breakage) are negligible compared to frictional mechanisms from local rearrangement of grains. In Tribology, the (static) coefficient of friction, μ, has essentially no upper limit for ideal metals that are thoroughly cleaned in dry vacuum (Hutchings, 1992), and this corresponds to a friction angle of $\phi = 90^\circ$. We might expect to have an increase of ω from 0 to 90° with ϕ increasing equally. However, when measured in air at room temperature with 50% relative humidity the values of μ are much smaller. The reduction in the coefficient of friction is because the smallest trace of oxygen or H_2O creates an oxide film along the contacting surfaces. The coefficient of friction of most metals would range between $\mu = 0.5$ and 1.5 (Ashby and Jones, 1980). Many metals, such as mild steel, are characterised by their ductility in shear deformation, where the shear stress–strain curve may be assumed, to a good order, as non-hardening perfectly plastic. We might expect that ductility will also appear in the compression of a system of metallic spheres, since although the boundary stresses are hydrostatic, the individual balls undergo significant microscopic shear. Therefore, although the exact correlation between ω and ϕ is uncertain, we believe that the $\omega-\phi$ relation should satisfy $\omega = 0^\circ$ when $\phi = 0^\circ$, growing up to $\omega = 90^\circ$ when μ increases to about 0.5–1.5 (i.e., $\phi = 26.5$–56.5°). In this setting, the ductile behaviour of a system of metallic balls will correspond to the extreme value of $\omega = 90^\circ$ (see Fig. 6). Let us assume for convenience the linear relationship

$$\omega = a\phi, \tag{56}$$

where a is introduced as an unknown constant. Since the extreme $\omega = 90^\circ$ should correspond to ϕ from 26.5° to 56.5°, a is expected to be in the range of 1.6–3.4. This assumption will be tested when comparing the theory with physical results, and providing a first estimation for a.

6. Comparison with physical results

Nakata et al. (2001) have provided sufficient details to examine the performance of the new theory in predicting sand behaviour under high pressure one-dimensional compression tests. Fig. 8 shows the evolution of grain size distribution curves of angular Silica sand with increasing vertical stress, plotted on a semi-logarithmic scale. The stress levels at which the grain sizes were measured are marked on an $e-\log(\sigma_v)$ plot in Fig. 9. As can be seen from the figure, the sand sample has an initial uniform grain size distribution with a maximum grain size of $d_M = 1.7$ mm and a minimum grain size of $d_{m0} = 1.4$ mm. This distribution remains more-or-less the same till the vertical stress exceeds a threshold of more than 9.6 MPa. From this point onwards the curves start to deviate from the initial distribution consistently towards an ultimate state. This ultimate distribution is unknown, but a fractal distribution may be a good starting point, as discussed in Part I (Einav, 2006). Such a theoretical ultimate fractal distribution is depicted in Fig. 8, for a fractal dimension of $\alpha = 2.55$.

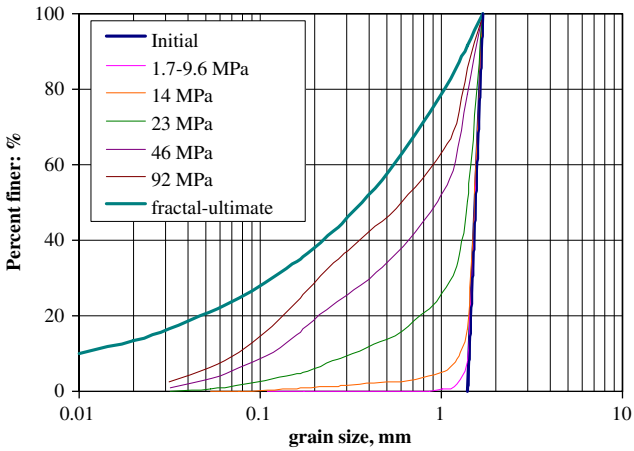

Fig. 8. Evolution of grain size distribution with applied vertical stress for uniformly graded sand under one-dimensional compression (after Nakata et al., 2001).

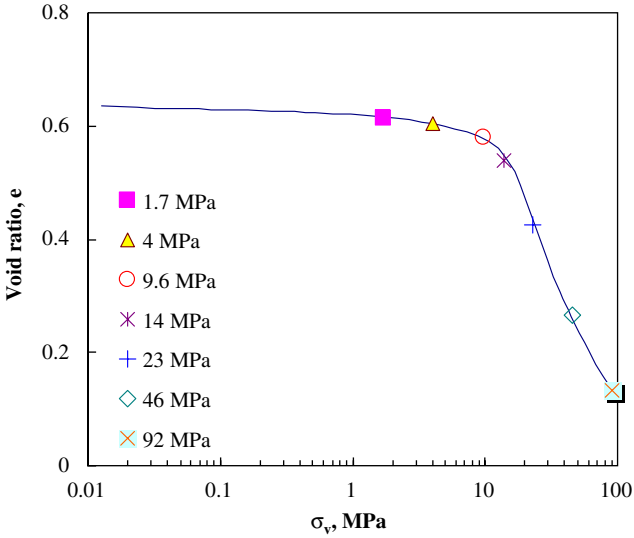

Fig. 9. An $e-\log(\sigma_v)$ plot of one-dimensional compression test on well graded sand (after Nakata et al., 2001).

For an initial uniform distribution with particles ranging from d_M down to d_{m0} (the 'originally' smallest grain size) J_{20} is given by

$$J_{20} = \frac{d_M^3 - d_{m0}^3}{3(d_M - d_{m0})}. \tag{57}$$

For $d_M = 1.7$ and $d_{m0} = 1.4\,\text{mm}$, $J_{20} = 2.41\,\text{mm}^2$, suggesting a reference grain size of $d_r = \sqrt{J_{20}} = 1.552\,\text{mm}$, which is nearly the average grain size. For an ultimate fractal distribution with $\alpha = 2.55$ and $d_M = 1.7\,\text{mm}$, Eq. (6) gives $J_{2u} = 0.312\,\text{mm}^2$. Using Eq. (3), $\vartheta = 0.87$.

The power function coefficient 'm' of the elastic relationship is assumed $^1/_2$ to represent the Hertzian contact law between particles. This in conjunction to the initial portion of the stress–strain curve suggests $\bar{K} = 4600$. For an initial yield stress of $p_{y0} = 7.3$ MPa, we find, using Eq. (17), that for this particular Silica sand the breakage strain energy constant should be around $G_B = 70.5$ kPa. The advantage as compared to conventional models, which use p_{y0} as a constant, is that G_B is independent of the initial void ratio e_0 and grain size distribution, while as noted by Nakata et al. (2001), p_{y0} is indeed dependent on these parameters. For an initial void ratio of $e_0 = 0.666$ and maximum void ratio of $e_{max} = 0.881$, Fig. 9 can be re-plotted as a stress–strain $p-e_v$ curve, or $e_v-\log(p)$ plot in Fig. 10, assuming that the lateral/axial effective stress ratio is $K_0 = 0.35$.

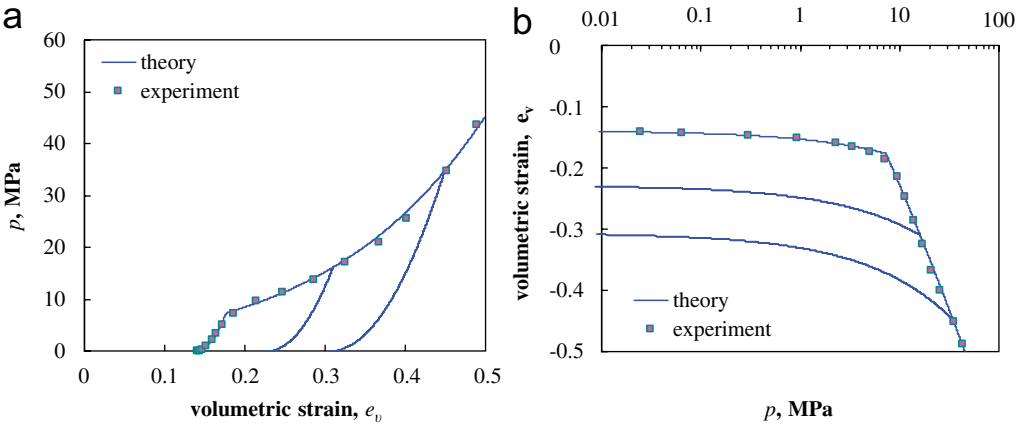

Fig. 10. 1D compression test on well graded sand (unloading cycles are predicted only using the theory): (a) p–e_v plot, and (b) an e_v–log(p) plot.

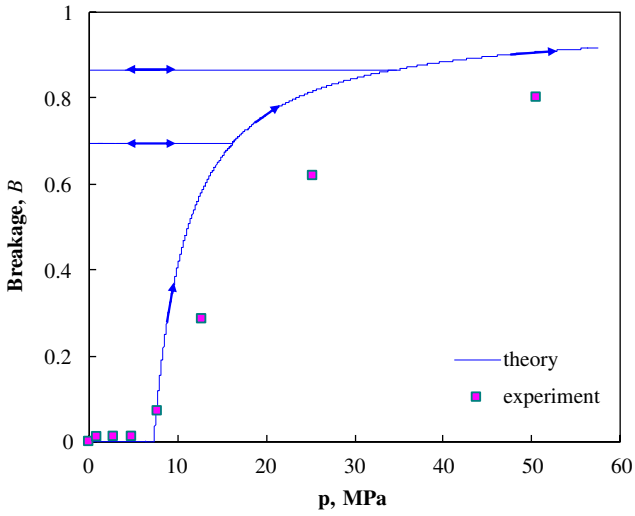

Fig. 11. The evolution of breakage during the 1D compression test: (a) p–e_v plot, (b) an e_v–log(p) plot.

The agreement between the theory and the experiment is excellent when the plastic-breakage coupling angle ω is 68°. Experience with angular Silica sand, such as the one used by Nakata et al. (2001), suggests a friction angle of about $\phi = 37°$ (personal communication with Airey, 2006) This, using Eq. (60) suggests that the constant $\alpha = 1.8$. A perfectly plastic behaviour would occur when $\omega = 90°$ and $\phi = 50°$, within the anticipated range of values.

The theoretical relation between the breakage and pressure, given by Eq. (55), can now be assessed. We measure the breakage, for the different stress levels, based on the experimental evolution of grain size distribution in Fig. 8, and the comparison is given in Fig. 11. The qualitative agreement is excellent, especially highlighting that no other physical theory has been proposed prior to this work to link between the breakage and the stress–strain behaviour of brittle granular materials.

7. Discussion on modelling shear deformations

Crushing of particles occurs in shear, as well as in compression. The above models were aimed for compression deformations only. During shear, localised shear bands may emerge to minimise energy by transmitting most of the velocity changes. When the particles are sufficiently 'strong', they may carry the excess normal micro forces that arise from the confined dilation. However, when the excess normal forces exceeds the particle strength, internal crushing begins. Hence, the ability to describe particles breakage directly via the constitutive relations should make an important research aim. The purpose of this section is only to pinpoint a possible direction for adding shear strains, rather than attempting to develop a definite model. This step of the paper is important for illustrating that the CBM theory may enable the derivation of complete models.

Within the framework of critical state soil mechanics, a general way to describe the dissipation in terms of shear and compression is given by (e.g., Collins and Houlsby, 1997)

$$\tilde{\Phi}_p = \frac{1}{2} p_y(\bullet)\sqrt{\delta e_v^{p2} + M^2 \delta e_s^{p2}}, \tag{58}$$

where e_s^p is the plastic shear strain, and M relates between the shear stress q and pressure p at failure conditions (i.e., $\eta_u \equiv q_u/p_u = M$), and is purely a function of the friction angle ϕ. Finally, $p_y(\bullet)$ is the pre-consolidation pressure, being a function of a variable '$\bullet$', which can be the plastic volumetric strain e_v^p, or the total volumetric strain e_v (Einav and Carter, 2007).

In relation to Section 4.3, the above dissipation may, in fact, be viewed to couple between the volumetric plastic dissipation $\tilde{\Phi}_p^{v*}$ and the shear plastic dissipation $\tilde{\Phi}_p^{s*}$, by representing (58) via

$$\Phi_p = \sqrt{\Phi_p^{v*2} + \Phi_p^{s*2}}, \tag{59}$$

with

$$\tilde{\Phi}_p^{v*} = \frac{1}{2} p_y(\bullet)\delta e_v^p, \tag{60}$$

$$\tilde{\Phi}_p^{s*} = \frac{1}{2} M p_y(\bullet)\delta e_s^p. \tag{61}$$

This highlights, however, an important limitation of conventional critical state models, where the overall dissipation ignores any fracture (or breakage) mechanisms.

This aspect could be rectified by employing the CBM formulation; for example, by adding an additional shear plastic term into the square root of Eq. (31), and accounting for (49) and (50)

$$\tilde{\Phi} = \sqrt{\sin^{-2}(\omega)\tilde{\Phi}_p^{v*2} + \cos^{-2}(\omega)\tilde{\Phi}_B^{*2} + \tilde{\Phi}_p^{s*2}} \geqslant 0. \tag{62}$$

This time, however, the individual terms $\tilde{\Phi}_p^{v*}$ and $\tilde{\Phi}_p^{s*}$ will take a different from Eqs. (60) and (61), unrelated to $p_y(\bullet)$. Instead, the individual dissipative components of the volumetric plastic term and the breakage term are taken in relation to (11) and (46):

$$\tilde{\Phi}_p^{v*} = \frac{\xi(e_v^e, e_s^e)}{\psi_r(e_v^e, e_s^e)} \frac{(1-\vartheta B)}{(1-B)^2} \frac{G_B}{\vartheta} \delta e_v^p, \tag{63}$$

$$\tilde{\Phi}_B^{*} = G_B(1-B)^{-2}\delta B \tag{64}$$

and the additional shear term is assumed by

$$\Phi_p^{s*} = M\xi(e_v^e, e_s^e)(1-\vartheta B)\delta e_s^p. \tag{65}$$

We note that $\psi_r(e_v^e, e_s^e)$ is now also a function of the elastic shear strain, and we designate $\xi(e_v^e, e_s^e) = \partial\psi_r(e_v^e, e_s^e)/\partial e_v^e$. The plasticity-breakage yield function is given by Legendre transformation:

$$y = \left(\sin(\omega)\frac{\vartheta\psi_r(e_v^e, e_s^e)E_B}{\xi(e_v^e, e_s^e)(1-\vartheta B)}p\right)^2 + (\cos(\omega)E_B)^2 + \left(\frac{G_B(1-B)^{-2}}{M\xi(e_v^e, e_s^e)(1-\vartheta B)}q\right)^2 - \frac{G_B^2}{(1-B)^4} \leqslant 0, \tag{66}$$

where the first term relates to plasticity in compression, second term to breakage, and third term to plasticity in shear. Since $p = \xi_v(e_v^e, e_s^e)(1-\vartheta B)$, $E_B = \psi_r(e_v^e, e_s^e)\vartheta$, and using the shear-pressure stress ratio $\eta = q/p$, the yield criterion may be re-written as

$$y \equiv \left(E_B(1-B)^2/G_B\right)^2 + \left(\eta/M\right)^2 - 1 \leqslant 0 \tag{67}$$

and the volumetric (63) and shear plastic dissipation (65) terms by

$$\tilde{\Phi}_p^{v*} = p\frac{G_B}{E_B(1-B)^2}\delta e_v^p, \tag{68}$$

$$\tilde{\Phi}_p^{s*} = Mp\delta e_s^p. \tag{69}$$

The deviation of Eq. (67) from the original breakage yield function in Eq. (10), via the extra term $(\eta/M)^2$ represents the fact that only in compression the breakage mechanisms could be referred to as 'active'. In this situation frictional dissipation emerges as a by-product of breakage dissipation. In shear the frictional dissipation is dominant but breakage appears inevitably from grains abrasion. This scenario represents a 'passive breakage mechanism'. We further note that the breakage growth criterion in Eq. (10)

follows any time the increment $d\eta = 0$ is zero. Finally, it should be highlighted that the current breakage model makes no use of the pre-consolidation term $p_y(\bullet)$. This concept is replaced by adopting the breakage energy constant. Here isotropic hardening is purely an emerging property of the breakage growth criterion rather than a curve-fitting exercise.

The shear dissipative term in Eq. (69) may be compared with the original term in Eq. (61). In ultimate state conditions the plastic work $\tilde{W}_p = p\delta e_v^p + q\delta e_s^p$ may be equated to the dissipation $\tilde{\Phi}$, implying that the elastic work is self-cancelled by the increment of change of the Helmholtz free energy, in view of Eq. (24). In terms of shear deformations, the ultimate state may be defined when both $\delta e_v^p = 0$ and $\delta B = 0$. In this situation, since both the breakage and compression dissipative terms are neglected, $q\delta e_s^p = \tilde{\Phi}_p^{s*}$, thus

$$\eta_u \equiv q_u/p_u = M \tag{70}$$

confirming with the Mohr–Coulomb failure criterion, and agreeing with the ultimate shear conditions that critical state soil mechanics predicts. Although only briefly explored, the above derivation proves the suitability of the CBM Theory in the modelling of shear deformations as well as compression.

8. Conclusions

The growth of breakage describes the evolution of the grain size distribution from an initial to ultimate distributions. In Part I (Einav, 2006) we incorporated the concept of breakage as an internal variable in a thermomechanical analysis and developed the theory for developing CBM models. The current work has furthered the theory to allow modelling materials that undergo plastic dissipation from the frictional rearrangement of particles in addition to the dissipation from breakage. The combination of the two dissipative mechanisms of breakage and plasticity was investigated. An important distinction is made, identifying two families of combined breakage-plasticity models. The first encompasses models with uncoupled plasticity and breakage yield surfaces. In this case, pure breakage can occur without plastic straining, or vice versa, pure plastic straining can happen without breakage. The second family describes models with a coupled breakage-plasticity yield surface, such that any plastic straining is accompanied to breakage.

Models are developed for brittle granular materials. The theory is validated against experiments. No other physical theory has been previously proposed that can link between the breakage and the stress–strain behaviour of brittle granular materials, although the breakage is frequently measured. The new Theory of CBM is capable to do that. For that purpose, a new average constant of granular material is defined, called the 'breakage strain energy constant', with which and a postulate of 'breakage growth', it is possible to explain the soil phenomenon of isotropic hardening directly from physical principles rather than from curve-fitting. This interpretation of hardening is rather different than the one used in classical critical state soil mechanics, and presented in a rather more rational-physical manner. The new interpretation has much in common with the interpretation given by McDowell et al. (1996) in what was termed as clastic hardening. However, the clastic hardening approach is limited for one dimensional compression loading conditions, and may not be derived from thermodynamics potentials. The CBM Theory, on the other hand, allows to develop models by following modern thermodynamics procedures, and the models are "complete" in the

sense that they can predict the material behaviour under different loading conditions. As an example, we have presented a simple model that may account for both shear and compression.

Appendix A. Elastic compression free energy in a reference grain fraction

A good approximation for the ensemble elastic behaviour of particulate aggregate may be given by a power function, representing the Hertzian contact law between particles (Walton, 1987). The elastic volumetric strain of granular materials that are initially compacted by a reference pressure p_r (conveniently taken as 1 kPa) may be assessed to a good order by using the following relation (Einav and Puzrin, 2004):

$$e_v^e - e_{v0} = \frac{(p/p_r)^{1-m} - 1}{\bar{K}(1-m)}, \tag{A.1}$$

where m and $\bar{K}$ are material constants; p is the mean effective stress, or effective pressure; e_v^e is the elastic volumetric strain; e_{v0} is a initial volumetric strain introduced to effectively describe the material dependence on the initial void ratio of the sample. A similar use of e_{v0} was undertaken by Einav and Carter (2007) for modelling clays. In sand, this measure may be linked to the maximum void ratio e_{max} which may be attained under the reference pressure of $p_r = 1$ kPa. This suggests that a universal zero strain is related to e_{max}. Of course, the initial void ratio e_0 may be that maximum value or less, depending on the amount of energy that is applied on the sample before returning to the reference pressure p_r. The connection between the volumetric strain e_v and void ratio e may be estimated by the incremental relation $de_v^e = de/(1+e)$. We evaluate e_{v0} as de_v^e, $de = e_{max} - e_0$ and we estimate the void ratio e, in the initial conditions, by the 'nominal initial void ratio' $e_{n0} = (e_0 + e_{max})/2$. This gives the following estimation of the initial volumetric strain $e_{v0} \approx (e_{max} - e_0)/(1 + e_{n0})$.

Differentiating Eq. (A.1) gives the elastic bulk modulus:

$$dp/de_v^e = \bar{K}(p/p_r)^m, \tag{A.2}$$

which effectively represents the Hertzian contact law between particles; in this case, experience shows that m would typically range between $^1/_3$ and $^1/_2$, and this is supported theoretically by Walton (1987); finally $\bar{K}$ depends on the intrinsic bulk and shear modulus of the grains, as well as the initial void ratio (or alternatively e_{v0}). The pressure as a function of volumetric strain is given by inverting (A.1):

$$p = \xi(e_v^e) = p_r \sqrt[1-m]{\bar{K}(1-m)(e_v^e - e_{v0}) + 1} \quad \text{for} \quad 0 \leqslant m < 1. \tag{A.3}$$

We note that when $m = 1$, the above model has a logarithmic limit,

$$p = \xi(e_v^e) = p_r \exp\left((e_v^e - e_{v0})/\kappa^*\right) \quad \text{for} \quad m = 1, \tag{A.4}$$

with $\kappa^* = 1/\bar{K}$ being the slope of the curve in the logarithmic space, as is normally assumed in critical state soil mechanics models. A linear (elastic) model is derived when $m = 0$, then $p - p_r = K(e_v^e - e_{v0})$, where $K = p_r\bar{K}$ would denote the conventional bulk modulus.

The above treatment does not account for the dependence of the material on the grain size distributions. To extend the above analysis we note, based on Eqs. $P_I(24)$ and $P_I(43)$,

that the Helmholtz free energy obtained by integrating Eqs. (A.3) and (A.4), is associated to the reference grain size:

$$\psi_r(e_v^e) = p_r \frac{\left(\xi(e_v^e)/p_r\right)^{2-m}}{\bar{K}(2-m)} \quad \text{for} \quad 0 \leqslant m < 1, \tag{A.5}$$

$$\psi_r(e_v^e) = p_r \kappa^* \exp\left((e_v^e - e_{v0})/\kappa^*\right) \quad \text{for} \quad m = 1. \tag{A.6}$$

The influence of the grain size distribution could now follow by combining either one of the above relations with the general expression in Eq. (1).

References

Airey, D.W., 2006. Personal communication.

Ashby, M.F., Jones, D.R.H., 1980. Engineering materials 1. An introduction to their properties and applications. International Series on Material Science and Technology. Pergamon Press.

Biarez, J., Hicher, P., 1994. Elementary Mechanics of Soil Behaviour. A.A. Balkema, Rotterdam.

Butterfield, R., 1979. A natural compression law for soils (an advance on e-logp'). Géotechnique 29 (4), 469–480.

Collins, I.F., Einav, I., 2005. On the validity of elastic/plastic decompositions in soil mechanics. Elastoplasticity. In: Tanaka, T., Okayasu, T. (Eds.), Proceedings of the Symposium on Elastoplasticity. Kyushu University, Japan, pp. 193–200.

Collins, I.F., Houlsby, G.T., 1997. Application of thermomechanical principles to the modeling of geomaterials. Proc. Royal Soc. London A 453, 1975–2001.

Einav, I., 2006. Breakage mechanics—Part I: theory. J. Mech. Phys. Solids (accepted, 9 October 2006), to be published.

Einav, I., Carter, J.P., 2007. On convexity, normality, pre-consolidation pressure and singularities of geomaterials. *Granul. Matter* 9(1–2) 87–96. (Available online http://dx.doi.org/10.1007/s10035-006-0025-z).

Einav, I., Puzrin, A.M., 2004. Pressure-dependent elasticity and energy conservation in elastoplastic models for soils. ASCE J. Geotech. Geoenviron. Eng. 130 (1), 81–92.

Hutchings, I.M., 1992. Tribology: Friction and Wear of Engineering Materials. Edward Arnold.

McDowell, G.R., Bolton, M.D., 1998. On the micromechanics of crushable aggregates. Géotechnique 48 (5), 667–679.

McDowell, G.R., Bolton, M.D., Robertson, D., 1996. The fractal crushing of granular materials. J. Mech. Phys. Solids 44 (12), 2079–2102.

Nakata, Y., Hyodo, M., Hyde, A.F.L., Kato, Y., Murata, H., 2001. Microscopic particle crushing of sand subjected to high pressure one-dimensional compression. Soils and Foundations 41 (1), 69–82.

Novello, E.A., Johnston, I.W., 1989. Normally consolidated behaviour of geotechnical materials. In: Proceedings of the 12th International Conference on Soil Mechanics, Rio de Janeiro, vol. 3. pp. 2095–2100.

Roscoe, K.H., Burland, J.B., 1968. Engineering Plasticity. In: Heyman, D., Leckie, D. (Eds.). Cambridge University Press, pp. 535–609.

Schofield, A.N., Wroth, C.P., 1968. Critical State Soil Mechanics. McGraw-Hill, London.

Walton, K., 1987. The effective elastic moduli of a random packing of spheres. J. Mech. Phys. Solids 35 (2), 213–226.